Loss Mechanisms of Optical Waveguides Inscribed in Fused Silica by Femtosecond Laser Direct Writing

Vítor A. Amorim, João M. Maia, Duarte Viveiros, and P. V. S. Marques

***Abstract*—Optical waveguides directly written in fused silica using a femtosecond laser were characterized from 350 to 1750 nm to gain insight on the waveguide's loss mechanisms and their dependence on processing parameters, such as pulse energy, scan velocity, and annealing temperature. Two major loss mechanisms were identified. In the range of parameters tested, high pulse energy was seen to improve coupling losses at long wavelengths, while high scan velocity has a negative effect in both Rayleigh scattering and coupling losses at long wavelengths. Thermal annealing of the waveguides demonstrated an improvement of the Rayleigh scattering at a cost of higher coupling losses at long wavelengths. Wavelength independent Mie scattering was also observed, evolving negatively with pulse energy. A minimum Rayleigh scattering coefficient of $\approx$0.5 dB$\cdot$cm$^{-1}\cdot\mu$m^4 ($\approx$0.08 dB$\cdot$cm$^{-1}\cdot\mu$m^4 for thermally treated waveguides) together with a Mie scattering coefficient of $\approx$0.2–0.65 dB/cm are reported.**

***Index Terms*—Annealing, coupling loss, femtosecond laser direct writing, heat treatment, integrated optics, Mie scattering, mode field mismatch, optical waveguides, propagation loss, Rayleigh scattering.**

I. Introduction

OPTICAL waveguides in the context of integrated optics have been traditionally fabricated by photolithographic techniques due to its technological maturity. However, a more recent approach relies on the use of a femtosecond laser to write the waveguide core directly in the material [1]. While photolithographic techniques offer significant advantages in scalability, cost, and circuit footprint, femtosecond laser direct writing can offer prototyping flexibility without the need for masks or multiple fabrication steps, and three-dimensional geometries that are not possible in traditional fabrication methods [2]. The latter has been used in several materials such as glasses, crystals, and polymers [2], and already enabled the fabrication of many integrated optical devices, including buried waveguides [3], Bragg grating waveguides [4], directional couplers [5], Y-junctions [6], integrated lasers [7], add-drop multiplexers [8], arrayed waveguide gratings [9], among others. Femtosecond laser direct writing can also benefit the ongoing exponential growth trend in data communications. The implementation of multicore fibers to scale the information transmitted by the number of cores, requires devices matching the out-of-plane characteristics of those fibers. It has been reported that this inherently 3D technique has already been implemented in the fabrication of three-dimensional fan-out devices for multicore fiber coupling applications [10]. On very specific materials, such as fused silica, this technique also enables the monolithic integration of optical waveguides together with microfluidic channels in a 3D fashion for on-chip optical sensing [11], [12]. Although infrared wavelengths are the most relevant for optical communications, shorter wavelengths are indeed important for applications like optical sensing relying on plasmonics or absorption measurements [13], [14]. Since shorter wavelengths are more affected by defects present in the waveguides [15], [16], understanding its loss mechanisms and their dependence with fabrication parameters is key to improve their quality as well as to maximize the performance of said devices.

In this paper, we report a systematic study of the spectral characteristics, from 350 to 1750 nm, of optical waveguides embedded in fused silica using femtosecond laser direct writing. Most of the studies present in the literature discuss waveguide loss around the 1550 nm region and, to the authors' knowledge, no such study exists on this extended wavelength range. In this work, several waveguides were written while varying pulse energy and scan velocity, with different heat treatments being also tested. Propagation and coupling losses were obtained from measuring the insertion loss of differently sized waveguides, giving definitive insight on the influence of the writing parameters and annealing temperature in both the Rayleigh and Mie scattering coefficients, as well as in the laser-induced refractive index modification combined with the waveguide dimensions. Such characterization improves our understanding on the dynamics of the scattering processes inherent to waveguides fabricated by femtosecond laser direct writing, and aids on the choice of the right fabrication parameters for a given application.

II. Experimental Procedure

A fiber amplified femtosecond laser (Amplitude Systèmes Satsuma HP), with a second harmonic beam at 515 nm and a pulse duration of approximately 250 fs at 500 kHz, was used

Manuscript received November 23, 2018; revised January 18, 2019; accepted February 18, 2019. Date of publication February 22, 2019; date of current version April 17, 2019. This work was supported in part by the Fundação para a Ciência e a Tecnologia through Grant SFRH/BD/128795/2017 and in part by Project "Coral - Sustainable Ocean Exploitation: Tools and Sensors/NORTE-01-0145-FEDER-000036," through the North Portugal Regional Operational Programme (NORTE 2020), under the PORTUGAL 2020 Partnership Agreement, and through the European Regional Development Fund (ERDF). *(Corresponding author: Vítor A. Amorim.)*

The authors are with the CAP—Centre for Applied Photonics, INESC TEC, Porto 4150-179, Portugal, and also with the Department of Physics and Astronomy, University of Porto, Porto 4169-007, Portugal (e-mail: vitor.a.amorim@inesctec.pt; joao.m.maia@inesctec.pt; carlos.d.viveiros@inesctec.pt; psmarque@fc.up.pt).

Color versions of one or more of the figures in this paper are available online at http://ieeexplore.ieee.org.

Digital Object Identifier 10.1109/JLT.2019.2900913

to induce the refractive index modification in pure fused silica substrates (Suprasil 1). Laser modification tracks were formed by transverse scanning the substrate on Aerotech air-bearing linear stages (ABL10100-LN), with the linearly polarized beam focused at a depth of 100 μm via a 0.55 numerical aperture aspherical lens (New Focus 5722-A-H) mounted in a vertical piezo stage (PI P-725.4CD PIFOC). Laser beam polarization was set parallel to the writing direction, and all waveguides were written on the same scanning direction to avoid the Quill effect [17].

The side facets of all substrates were polished after writing in order to eliminate laser damage induced in the substrates' input and output facets, and to remove the waveguide tapered region created by the influence of the substrates' edge on the beam focus.

To determine the spectral characteristics of the fabricated devices, the broad spectrum of a halogen lamp was coupled into a single-mode fiber (SMF-28) and butt-coupled to the entrance facet of the modification tracks. The substrate was mounted on an Elliot Martock MDE881 stage with piezo controls (Dali E-2100) and special holders for precise alignment of the input/output optical fibers. The light collected by a second butt-coupled optical fiber at the exit facet was inspected in an optical spectrum analyzer (ANDO AQ-6315B) from 350 nm to 1750 nm with a 10 nm resolution. All transmission spectra were normalized to the source spectrum to obtain the insertion loss. Index matching (Cargille series: AA $\mathrm{n_D^{25^\circ C}} = 1.458 \pm 0.0002$) was used to minimize Fresnel reflections at both input/output fibers/facets.

Sample annealing, when employed, was made during 2 hours at the target annealing temperature, using a 15 °C/min heating ramp, on a Carbolite RHF 1500 furnace.

III. Experimental Results and Discussion

For this study several sets of waveguides were fabricated in a 75 mm long fused silica substrate with a pulse energy and scan velocity ranging from 50 nJ to 400 nJ and 100 μm/s (doubling after each waveguide) to 6400 μm/s, respectively. These sets were replicated and used to test the spectral characteristics of the waveguides after a thermal treatment at 800, 900, 1000, and 1200 °C.

Fig. 1 displays the cross-section and top views of waveguides fabricated with different pulse energies for a scan velocity of 100 μm/s and 3200 μm/s. The elongated modification, with a decreased refractive index at the top followed by a bottom guiding region, is typical for fused silica when employing transverse scanning [18]. As shown, the modified volume dimensions increase significantly with pulse energy, diminishing slightly at high scan velocities. Furthermore, waveguide rugosity becomes more pronounced at greater pulse energies, becoming more apparent at high scan velocities (Fig. 1, top view).

The spectral characteristics of optical waveguides fabricated by femtosecond laser direct writing also depend on pulse energy and scan velocity, as can be seen in Fig. 2(a) and (b) respectively. In the first case, the insertion losses at long wavelengths become smaller as pulse energy increases, while in the second

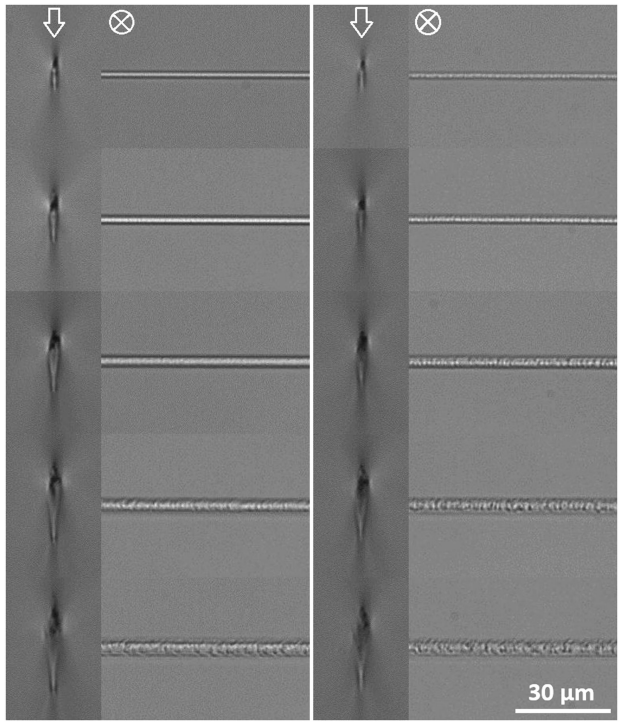

Fig. 1. Transmission mode optical microscope images of the cross-section and top views of waveguides written in fused silica with pulse energies of 50, 100, 200, 300, and 400 nJ (top to bottom, respectively), for a scan velocity of 100 μm/s (left) and 3200 μm/s (right). Arrows indicate the laser beam propagation direction.

they increase as scan velocity increases. At short wavelengths, however, insertion loss shows no clear dependence with pulse energy, increasing again for higher scan velocities. Apparently, this behaviour at shorter wavelengths can be counteracted with annealing, as seen in Fig. 2(c), where insertion loss decreases with increasing annealing temperature. The same behaviour was observed by Bhardwaj *et al.* at 633 nm [19]. Despite this improvement, there is a trade-off, since the insertion loss at long wavelengths increases at higher annealing temperatures. From the gathered data, the behaviour described here occurs for all parameters under study in the range tested. Waveguides fabricated with a scan velocity of 6400 μm/s as well as waveguides annealed at 1200 °C were not considered in this study due to the very weak light guidance.

To better understand the processes underlying the spectral behaviour, the cut-back technique was used. In this study the substrates were diced into three different lengths (1.3, 2.2, and 3.3 ± 0.1 cm), with the insertion loss of each waveguide being plotted, with the aid of a python program, as a function of sample length for each wavelength. Using the Levenberg-Marquardt algorithm, a linear fit employing equation (1) was able to retrieve both propagation (slope) and coupling loss (y-axis interception) within the wavelength range studied in this work, as shown in Fig. 2(d).

$$IL(\lambda) = PL(\lambda) \times L + 2CL(\lambda) \tag{1}$$

Fig. 3 displays the obtained coupling and propagation losses. From Fig. 3(a–c), it is possible to see that there are three main

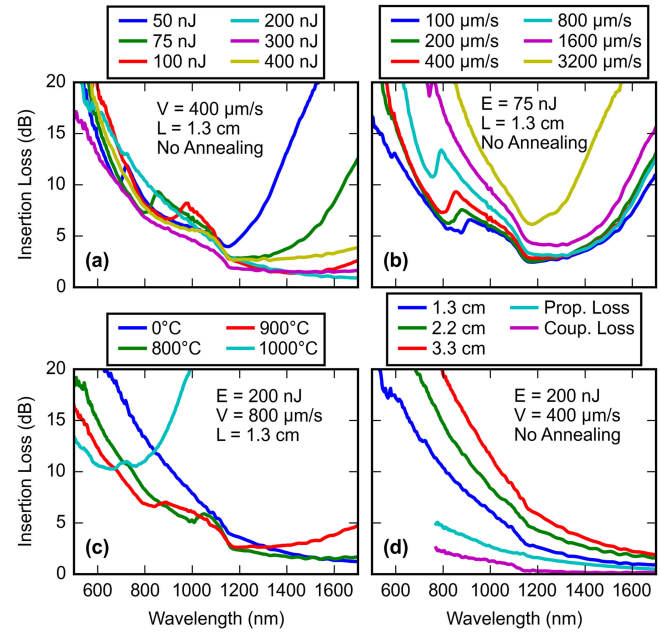

Fig. 2. Insertion loss of the fabricated waveguides as a function of wavelength for varying pulse energy (a), scan velocity (b), and annealing temperature (c). (d) Insertion loss of a waveguide for different lengths, together with propagation and coupling loss plotted in dB/cm and dB/facet, respectively.

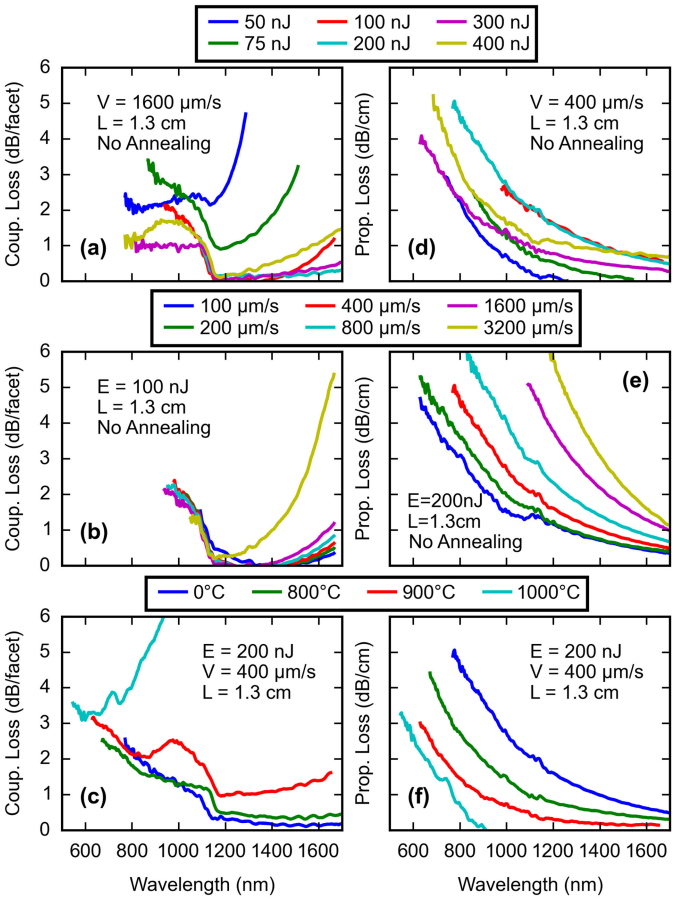

Fig. 3. Coupling and propagation loss of the fabricated waveguides as a function of wavelength for varying pulse energy (a, d), scan velocity (b, e), and annealing temperature (c, f).

occurrences of interest. The first is the immediate increase in coupling losses at approximately 1150 nm; at this wavelength the butt-coupling fibers become multimode, increasing the mode mismatch and, therefore, the coupling losses. The second is the monotonic growth in coupling losses, at longer wavelengths, as wavelength increases. This originates from the decrease in V-number [20], given by:

$$V = \frac{2\pi}{\lambda} a \sqrt{n_{core}^2 - n_{substrate}^2}, \tag{2}$$

where a is generally the waveguide core radius, and λ the signal wavelength, leading the guiding conditions closer to the cut-off condition and, therefore, increasing the mode field diameter, which translates into additional mode mismatch. The third occurrence of interest is the variation in coupling losses, at longer wavelengths, with the tested parameters. We conclude that, at long wavelengths, coupling losses increase whenever the pulse energy is decreased, the scan velocity increased, or when the annealing temperature at which the waveguides were submitted is higher. Previous studies evidenced the creation of nonbridging oxygen hole centers and self-trapped exciton (E'_g) defects along with increased 3- and 4-membered rings in the silica network of femtosecond laser written waveguides. The increased 3- and 4-membered rings' concentration in the silica network are associated with material densification and are responsible for the higher refractive index, which increases with pulse energy [21]–[25]. While defects anneal out at a temperature as low as 150 °C, the increase in 3- and 4-membered rings' concentration is significantly more resistant to thermal treatment, only annealing out after heat treatment at 800–900 °C for long periods of time [26], [27]. These results match our observations, since a lower refractive index contrast together with lower physical waveguide dimensions, deriving from a smaller net writing fluence and/or higher annealing temperature, reduces the V-number, thereby increasing mode field diameter and, subsequently, mode mismatch, as it has already been observed by Shah *et al.* at 1550 nm [28]. This demonstrates the importance of the fabrication and heat treatment parameters in the guidance characteristics at long wavelengths, since low pulse energy, high scan velocity, and/or high annealing temperatures will lead to low quality waveguides in this region. It should be also taken into consideration that the coupling loss reflects the overlap integral of the optical modes propagating in the written waveguide with the input/output optical fiber mode, meaning that employing different optical fibers will result in different coupling loss results.

In Fig. 3(d–f), the monotonic increase in propagation loss, as wavelength decreases, is visible for all fabrication parameters tested. This behaviour was already observed by Thomson *et al.*, where a higher propagation loss was observed at 640 nm when compared to 980 nm; this was attributed to the possibility of loss being dominated by Rayleigh scattering [15]. Scattering plays a major role on femtosecond laser written waveguides, as has been also shown by Tong *et al.*, where it accounts for more than 90% of the propagation loss at 633 nm [16]. The C/λ^4 trend observed in Fig. 3(d–f) suggests a strong Rayleigh scattering influence in propagation loss, possibly created by sub-wavelength inhomogeneities in the refractive index of the waveguides dur-

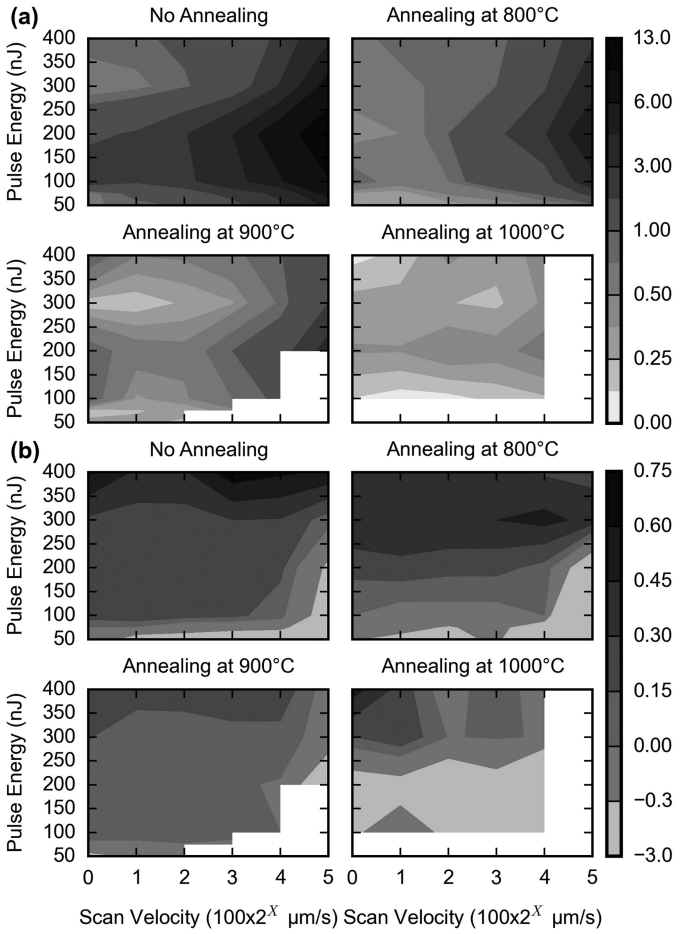

Fig. 4. Rayleigh (a) and Mie (b) scattering coefficients, in $\mathrm{dB \cdot cm^{-1} \cdot \mu m^4}$ and dB/cm respectively, as a function of pulse energy and scan velocity for the different annealing temperatures.

ing the writing process. As can be seen, no particular behavior is evident when the pulse energy is varied. However, when the scan velocity increases, the propagation loss steepens, meaning that the Rayleigh scattering coefficient rises. The aforementioned behavior can be counteracted by applying thermal treatments, as detailed in Fig. 3(f). Despite Rayleigh scattering being the major contributor to propagation loss, an almost wavelength independent baseline loss also exists, which was attributed to Mie scattering.

The propagation loss data was modelled using equation (3) together with a python program employing the Levenberg-Marquardt algorithm to fit the Rayleigh and Mie scattering coefficients (C_{RS} and C_{MS}, respectively).

$$PL = \frac{C_{RS}}{\lambda^4} + C_{MS} \tag{3}$$

The Rayleigh and Mie scattering coefficients, obtained from the fabricated waveguides' propagation loss fittings, are plotted in Fig. 4. Rayleigh scattering is seen to increase with scan velocity for all pulse energies tested, from a minimum of ≈0.5 to a maximum of 12.4 $\mathrm{dB \cdot cm^{-1} \cdot \mu m^4}$. This tendency is successfully attenuated by applying thermal treatments at increasingly higher temperatures, with improvements being found even at low scan velocities. A minimum Rayleigh scattering coefficient of approximately 0.08 $\mathrm{dB \cdot cm^{-1} \cdot \mu m^4}$ was found after a thermal treatment at 1000 °C. Pulse energy dependent behavior is also present, with higher Rayleigh scattering coefficients being found in waveguides fabricated at 200 nJ, independently of the annealing temperature. The absence of data at high annealing temperatures, low pulse energies, and high scan velocities, is due to the low light guidance resulting from the increasing scattering and coupling losses. The extracted Mie scattering coefficients are plotted in Fig. 4(b). A negative region is present whenever the scan velocity is high and pulse energy low, growing for higher annealing temperatures; this is clearly unrealistic and arises from the lack of a nearly constant spectral component at long wavelengths, since, in these cases, the fitting is made with rapidly varying propagation loss data. On the other hand, an increase in the Mie scattering coefficient of ≈0.2 to 0.65 dB/cm is seen as pulse energy increases, being relatively independent of scan velocity. This behavior suggests that Mie scattering most likely arises from an energy dependent process. However, as seen in Fig. 1, micron scale inhomogeneities created within the waveguide become more apparent at higher pulse energy and scan velocity. This contradiction in scan velocity dependence most likely arises from the absence of a slowly varying spectral content at longer wavelengths, as discussed above. Occasional defects created by dust on the substrates' surface, glass non-uniformities, and vibrations of the fabrication setup could also further explain the origin of the scattering mechanisms. An improvement of the Mie scattering coefficients can be achieved, to some extent, through thermal processing.

The results obtained here are comparable to those achieved by Eaton *et al.* in Eagle2000 substrates, whose Rayleigh scattering coefficient ranged between 0.8 to 1.7 $\mathrm{dB \cdot cm^{-1} \cdot \mu m^4}$ and Mie scattering coefficient was around 0.16 dB/cm [29]. These authors found that the Mie scattering was independent of scan velocity and that the Rayleigh scattering decreases for higher scan velocity. This difference may arise not only from the glass used but also from the very limited number of waveguides tested. The different type of glass substrate also meant a two orders of magnitude higher scan velocity compared to our case for a similar Rayleigh scattering.

There is no doubt that further exploration of fabrication variables is required to reduce the $10^4 - 10^5$ fold higher Rayleigh scattering coefficient of femtosecond laser written waveguides when compared to silica-core single-mode fibers [30]. Variables such as the writing laser's pulse front tilt, spatial beam profile, astigmatism, polarization state, pulse duration, repetition rate, and others, such as the lens numerical aperture, still present the opportunity for future developments in the guiding characteristics of waveguides fabricated by femtosecond laser direct writing.

IV. Conclusion

The guiding properties of waveguides fabricated by femtosecond laser direct writing in fused silica substrates were tested while varying processing parameters such as pulse energy, scan velocity, and annealing temperature. The insertion losses of such waveguides presented a mid-wavelength guiding

band limited by increasingly higher losses at long and short wavelengths. Coupling losses were found to control the long wavelength behaviour, with its monotonic growth, as wavelength increases, arising from an increasing mode mismatch. Furthermore, coupling losses increased whenever the pulse energy decreased, the scan velocity increased, or when the annealing temperature at which the waveguides were submitted was higher. The short wavelength behaviour followed a C/λ^4 trend in propagation loss, suggesting a strong Rayleigh scattering influence. Rayleigh scattering was seen to increase with scan velocity from $\approx$0.5 to 12.4 $\mathrm{dB \cdot cm^{-1} \cdot \mu m^4}$, being attenuated with the application of thermal treatments, reaching a minimum of $\approx$0.08 $\mathrm{dB \cdot cm^{-1} \cdot \mu m^4}$ when treated at 1000 °C. An almost wavelength independent baseline loss was also observed, which was attributed to Mie scattering. The former showed to be relatively independent of scan velocity, increasing from $\approx$0.2 to 0.65 dB/cm as pulse energy increased.

Future developments of the overall spectral characteristics of waveguides fabricated by femtosecond laser direct writing should be possible with further exploration of other fabrication parameters and post-fabrication treatment conditions.

REFERENCES

[1] K. M. Davis, K. Miura, N. Sugimoto, and K. Hirao, "Writing waveguides in glass with a femtosecond laser," *Opt. Lett.*, vol. 21, no. 21, pp. 1729–1731, Nov. 1996.

[2] G. D. Valle, R. Osellame, and P. Laporta, "Micromachining of photonic devices by femtosecond laser pulses," *J. Opt. A, Pure Appl. Opt.*, vol. 11, no. 1, Dec. 2008, Art. no. 013001.

[3] S. M. Eaton, H. Zhang, and P. R. Herman, "Heat accumulation effects in femtosecond laser-written waveguides with variable repetition rate," *Opt. Express*, vol. 13, no. 12, pp. 4708–4716, Jun. 2005.

[4] H. Zhang, S. M. Eaton, and P. R. Herman, "Single-step writing of Bragg grating waveguides in fused silica with an externally modulated femtosecond fiber laser," *Opt. Lett.*, vol. 32, no. 17, pp. 2559–2561, Sep. 2007.

[5] S. M. Eaton *et al.*, "Telecom-band directional coupler written with femtosecond fiber laser," *IEEE Photon. Technol. Lett.*, vol. 18, no. 20, pp. 2174–2176, Oct. 2006.

[6] V. A. Amorim, J. M. Maia, D. Alexandre, and P. V. S. Marques, "Optimization of broadband Y-junction splitters in fused silica by femtosecond laser writing," *IEEE Photon. Technol. Lett.*, vol. 29, no. 7, pp. 619–622, Apr. 2017.

[7] T. Calmano, J. Siebenmorgen, O. Hellmig, K. Petermann, and G. Huber, "Nd:YAG waveguide laser with 1.3 W output power, fabricated by direct femtosecond laser writing," *Appl. Phys. B*, vol. 100, no. 1, pp. 131–135, Jul. 2010.

[8] V. A. Amorim, J. M. Maia, D. Alexandre, and P. V. S. Marques, "Monolithic add-drop multiplexers in fused silica fabricated by femtosecond laser direct writing," *J. Lightw. Technol.*, vol. 35, no. 17, pp. 3615–3621, Sep. 2017.

[9] G. Douglass, F. Dreisow, S. Gross, and M. J. Withford, "Femtosecond laser written arrayed waveguide gratings with integrated photonic lanterns," *Opt. Express*, vol. 26, no. 2, pp. 1497–1505, Jan. 2018.

[10] R. R. Thomson *et al.*, "Ultrafast-laser inscription of a three dimensional fan-out device for multicore fiber coupling applications," *Opt. Express*, vol. 15, no. 18, pp. 11691–11697, Sep. 2007.

[11] J. M. Maia, V. A. Amorim, D. Alexandre, and P. V. S. Marques, "Real-time optical monitoring of etching reaction of microfluidic channel fabricated by femtosecond laser direct writing," *J. Lightw. Technol.*, vol. 35, no. 11, pp. 2291–2298, Jun. 2017.

[12] A. Crespi *et al.*, "Three-dimensional Mach-Zehnder interferometer in a microfluidic chip for spatially-resolved label free detection," *Lab Chip*, vol. 10, no. 9, pp. 1167–1173, May 2010.

[13] C. Caucheteur, T. Guo, and J. Albert, "Review of plasmonic fiber optic biochemical sensors: improving the limit of detection," *Analytical Bioanalytical Chem.*, vol. 407, no. 14, pp. 3883–3897, May 2015.

[14] M. Kim, D. J. Hwang, H. Jeon, K. Hiromatsu, and C. P. Grigoropoulos, "Single cell detection using a glass-based optofluidic device fabricated by femtosecond laser pulses," *Lab Chip*, vol. 9, no. 2, pp. 311–318, Jan. 2009.

[15] R. R. Thomson *et al.*, "Active waveguide fabrication in erbium-doped oxyfluoride silicate glass using femtosecond pulses," *Appl. Phys. Lett.*, vol. 87, Sep. 2005, Art. no. 121102.

[16] L. Tong, R. R. Gattass, I. Maxwell, J. B. Ashcom, and E. Mazur, "Optical loss measurements in femtosecond laser written waveguides in glass," *Opt. Commun.*, vol. 259, pp. 626–630, Mar. 2006.

[17] P. G. Kazansky *et al.*, "Quill writing with ultrashort light pulses in transparent materials," *Appl. Phys. Lett.*, vol. 90, no. 15, Apr. 2007, Art. no. 151120.

[18] H. Huang, L. Yang, and J. Liu, "Femtosecond fiber laser direct writing of optical waveguides in glasses," *Proc. SPIE*, vol. 8164, Aug. 2011, Art. no. 81640B.

[19] V. R. Bhardwaj, P. B. Corkum, D. M. Rayner, C. Hnatovsky, E. Simova, and R. S. Taylor, "Stress in femtosecond-laser-written waveguides in fused silica," *Opt. Lett.*, vol. 29, no. 12, pp. 1312–1314, Jun. 2004.

[20] D. Gloge, "Weakly guiding fibers," *Appl. Opt.*, vol. 10, no. 10, pp. 2252–2258, Oct. 1971.

[21] J. W. Chan, T. Huser, S. Risbud, and D. M. Krol, "Structural changes in fused silica after exposure to focused femtosecond laser pulses," *Opt. Lett.*, vol. 26, no. 21, pp. 1726–1728, Nov. 2001.

[22] J. W. Chan, T. R. Huser, S. H. Risbud, and D. M. Krol, "Modification of the fused silica glass network associated with waveguide fabrication using femtosecond laser pulses," *Appl. Phys. A*, vol. 76, no. 3, pp. 367–372, Mar. 2003.

[23] W. J. Reichman *et al.*, "A spectroscopic comparison of femtosecond-laser-modified fused silica using kilohertz and megahertz laser systems," *J. Appl. Phys.*, vol. 99, no. 12, Jul. 2006, Art. no. 123112.

[24] D. J. Little, M. Ams, P. Dekker, G. D. Marshall, J. M. Dawes, and M. J. Withford, "Femtosecond laser modification of fused silica: the effect of writing polarization on Si-O ring structure," *Opt. Express*, vol. 16, no. 24, pp. 20029–20037, Nov. 2008.

[25] M. Sakakura, M. Terazima, Y. Shimotsuma, K. Miura, and K. Hirao, "Thermal and shock induced modification inside a sílica glass by focused femtosecond laser pulse," *J. Appl. Phys.*, vol. 109, no. 2, Feb. 2011, Art. no. 023503.

[26] A. Champion and Y. Bellouard, "Direct volume variation measurements in fused silica specimens exposed to femtosecond laser," *Opt. Mater. Express*, vol. 2, no. 6, pp. 789–798, May 2012.

[27] J. J. Witcher, W. J. Reichman, L. B. Fletcher, N. W. Troy, and D. M. Krol, "Thermal annealing of femtosecond laser written structures in silica glass," *Opt. Mater. Express*, vol. 3, no. 4, pp. 502–510, Mar. 2013.

[28] L. Shah, A. Y. Arai, S. M. Eaton, and P. R. Herman, "Waveguide writing in fused silica with femtosecond fiber laser at 522 nm and 1 MHz repetition rate," *Opt. Express*, vol. 13, no. 6, pp. 1999–2005, Apr. 2005.

[29] S. M. Eaton *et al.*, "Spectral loss characterization of femtosecond written waveguides in glass with application to demultiplexing of 1300 and 1550 nm wavelengths," *J. Lightw. Technol.*, vol. 27, no. 9, pp. 1079–1085, May 2009.

[30] H. Kanamori *et al.*, "Transmission characteristics and reliability of pure-silica-core single-mode fibers," *J. Lightw. Technol.*, vol. LT-4, no. 8, pp. 1144–1150, Aug. 1986.

Vítor A. Amorim received the B.Sc. degree in technological physics and the M.Sc. degree in physical engineering from the University of Porto, Porto, Portugal. Since 2016, he has been working toward the Ph.D. degree in physics with the University of Porto. He joined the Centre for Applied Photonics, INESC TEC, Porto, Portugal, in 2015, where he is currently enrolled in research activity. His current research interests include integrated optical devices and monolithic optofluidic devices fabricated by femtosecond laser direct writing for sensing applications.

João M. Maia received the B.Sc. degree in technological physics and the M.Sc. degree in physics engineering, both from the Faculty of Sciences, University of Porto, Porto, Portugal, in 2014 and 2016, respectively. Since September 2016, he has been a student of the Physics doctoral programme with the University of Porto. In 2015, he joined the Centre for Applied Photonics (CAP), INESC TEC, Porto, Portugal, where he is currently doing research on femtosecond laser micromachining. His current research interests cover fabrication of optofluidic devices for chemical sensing and photopolymerization.

Duarte Viveiros was born in Machico, Madeira, Portugal, in 1990. He received the B.Sc. degree in electronics and telecommunications engineering and the M.Sc. degree in energy networks and telecommunications engineering from the University of Madeira, Funchal, Portugal, in 2011 and 2013, respectively. Since 2015, he has been a student with the Physics and Astronomy Department, Faculty of Sciences, Porto University, Porto, Portugal, involved in the joint Doctoral MAP-fis programme.

In 2013, he joined the Centre for Applied Photonics (CAP), INESC TEC, Porto, Portugal, where he was a Research Assistant with the European project ECOAL – MGT – SOE3/P2/P714, Ecological Management of Coal Waste Piles in Combustion, as a part of the SUDOE – Interreg IV B programme. His current research interests and activities focus on optical fiber sensing technology and integrated optics systems: three-dimensional (3D) micro-/nanofabrication based on femtosecond laser mechanisms; femto-etching and direct writing micromachining fabrication methods; design and fabrication of novel fibre optic and integrated optics sensor devices; test and optimization of selected sensors in practical applications; and remote and distributed sensing.

Mr. Viveiros is a member of the University of Porto SPIE Student Chapter, SPIE - International Society for Optics and Photonics.

P. V. S. Marques is an Associate Professor with the Physics and Astronomy Department, Faculty of Sciences, Porto University, Porto, Portugal, and since October 2009, he has been the Coordinator of the Center of Applied Photonics, INESCTEC, Porto, Portugal, and also the Director of the Micro and Nanofabrication Center of Porto University (CEMUP MNTEC), Porto, Portugal.

His current research interests include optical sensors, femtosecond laser direct writing techniques for integrated optics and microfabrication in general, microfluidics, Bragg gratings and active devices. He has authored and co-authored four world patents (patent family of 32), more than 100 scientific papers in international magazines and conferences, and three book chapters.